Single image summary of time-varying Earth-features

Gaurav Tripathi

Masters student
University of Calgary
Department of Computer
Science
Calgary, AB T2N 1N4,
Canada
gaurav.tripathi@ucalgary.ca

Katayoon Etemad

Postdoctoral Fellow
University of Calgary
Department of Computer
Science
Calgary, AB T2N 1N4,
Canada
ketemad@ucalgary.ca

Faramarz Samavati

Full Professor
University of Calgary
Department of Computer
Science
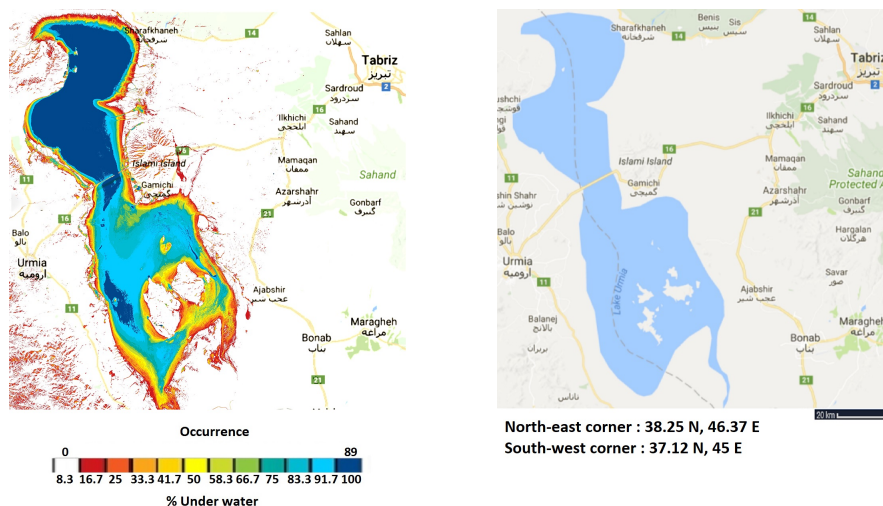Calgary, AB T2N 1N4,
Canada
samavati@ucalgary.ca

Figure 1: Lake Urmia 89 layers SIS from 2013-2017.

ABSTRACT

The Earth's surface is live and dynamic due to natural and manmade events. Tracking and visualizing Earth-features (e.g. water, snow, and vegetation) is an important problem. Earth observation satellite imagery like Landsat 8 makes the tracking feasible by providing detailed multispectral imagery at regular intervals. In this paper, we explore a single image summary approach to detecting changes in Earth-features by using the Landsat 8 dataset. In our system, we use appropriate thresholds for spectral indices to identify features, reference datasets, and combine multiple images using predefined color palettes to generate a single image summary of features for a region. Furthermore, we illustrate the benefit of our method over traditional visualizations with case-studies for the Lake Urmia, the Amazon Rainforest, and the Bering Glacier.

Keywords

Visualization, Remote sensing, Landsat 8, Spectral indices, Deforestation, Drought, Glacial melting

1 INTRODUCTION

Earth is dynamic and ever-changing planet. Natural resource managers, policymakers, researchers, and, the general public need information about these changes to

detect environmental changes and assess the impacts of global warming [30]. Displaying a video or scientific charts are useful but not sufficient to clearly show the changes in the *Earth-features* (e.g. Vegetation, water, snow) present on the Earth's surface, due to phenomenon like desiccation of lakes, melting of glaciers, and deforestation. Changes in individual Earth-features are not always visible in regular RGB images. Moreover, it is hard to perceive significant changes in a short period of time. Capturing changes in the Earth-features and visualizing them in an appropriate way is a fundamental and important problem.

The regular collection of datasets performed by Earth observation satellites can play an important role in addressing the issue of capturing Earth-feature changes. In this paper, we use Landsat 8 satellite imagery datasets to identify and detect changes in Earth-features. In addition to regular RGB images, Landsat 8 data contains spectral bands (i.e. a range of frequencies along the electromagnetic spectrum) that can reveal important features of a region such as the prevalence of snow, water, and vegetation.

With respect to the visualization challenge, techniques like animated timelapses and image lineups are traditionally used. These techniques are used to represent temporal changes in Earth-features. One major problem with the animated timelpase approach, like Google Timelapse [11], is the loss of context. To identify Earth-feature changes using a video, the observer needs to move back and forth between video frames. In the second traditional approach, a number of images are placed side-by-side to allow for comparisons between multiple frames. The main drawback to the use of multiple images on screen (or on paper) is that the size of the individual images needs to be reduced to fit all of them in a single frame. The size reduction results in detail loss for high-resolution images, and is especially pronounced when there are many images. "small multiples large singles" mentioned in [35] is in congruence to using SIS and making it convenient for users to perform effective visual exploration.

To address the limitations of these traditional techniques, in this paper, we propose a novel single image summary (*SIS*) for Earth-features using Landsat 8 images (e.g. Figure 1). SIS represents temporal changes to the Earth-features in a given region over a fixed duration of time. To create a SIS, we determine the Earth-feature recurrence, e.g. water existence, for any location in the region of interest (ROI) and then map the resulting recurrence values to predefined colors. To provide a better context for the feature of interest, we call this location-based recurrence distribution a *recurrence map*. We also add an overlay of the traditional map of the surrounding areas. SIS representation resolves the loss of context issue and retains the resolution of the original image dataset.

To prepare a SIS, we download data for a region covering the duration of interest. The cloudy pixels are detected using the Quality Assurance band provided by Landsat 8. In the next step, relevant Earth-features are identified by using spectral band operations. After feature identification, we generate the recurrence map by counting the occurrence of that feature in every location in the region. To facilitate these operations, and as a proof of concept, we have implemented a software prototype. In our system, we use the recurrence map and predefined color palettes to generate single image summaries for three Earth-features: vegetation, water, and snow. We

use our system in three case studies : (i) Lake Urmia , (ii) the Amazon Rainforest, and, (iii) the Bering Glacier. We also discuss the impact of different color palettes on results.

The paper is arranged as follows. Section 2 covers previous work and related material on Landsat 8, spectral indices and geospatial visualization. Section 3 details our approach and implementation. Section 4 discusses the case-studies. Section 5 concludes this article and suggests future works.

2 BACKGROUND AND RELATED WORK

2.1 Landsat 8

For over 40 years, seven Landsat satellites have collected spectral information regarding the Earth's surface. The latest satellite dataset in the series, Landsat 8, was made available for free public use on May 30, 2013 [30]. The near polar orbit of Landsat 8 allows it to regularly visit an area every 16 days. This temporal resolution allows researchers to track seasonal changes on the Earth's surface, as in this work, which tracks changes in time-varying Earth-features. The Landsat 8 sensors collect data at a spatial resolution of 30 meters (visible, NIR, SWIR); 100 meters (thermal); and 15 meters (panchromatic).

Landsat 8 measures the energy reflected by land surface across different frequency ranges from the electromagnetic spectrum. Each range of frequency is called a band. Land features like water, vegetation, and snow reflect energy based on their unique surface characteristics. Thus, measuring reflected energy helps one identify the observed feature. In multispectral satellite imagery, multiple band data is used to create spectral indices that make it possible to identify features. The Green (0.533 - 0.590 micrometers), Red (0.636 - 0.673 micrometers), Near-infrared (0.851 - 0.879 micrometers), and Shortwave infrared (1.566 - 1.651 micrometers) bands have been used in this research. These bands are combined to create metrics that assist in discriminating Earth-features.

2.2 Spectral Indices

A spectral index is a metric used to identify specific features or phenomena in remote sensing imagery. It is prepared by linear or nonlinear combinations of two or more bands. Vegetation, water, and snow indices are one of the most studied and commonly used spectral indices [37] in the field of remote sensing. An optimally designed spectral index is supposed to be as sensitive as possible to the essential feature of interest and insensitive to nonessential features in the observation area [36]. In this paper, we particularly focus on spectral indices for vegetation, water, and snow.

The normalized difference vegetation index (NDVI) is a spectral index that can be used to analyze remote sensing measurements and assess whether the target contains live green vegetation [26, 29]. Live vegetation absorbs solar radiation in the photosynthetically active range with a wavelength between 400 to 700 nanometers. Wavelengths up to red can be used by leaves to synthesize organic molecules while NIR and longer wavelengths cannot be used for synthesis. Hence, the leaves reflect energy of the NIR range. NDVI utilizes these facts in a simple form as

$$NDVI(p) = \frac{NIR(p) - Red(p)}{NIR(p) + Red(p)} \tag{1}$$

where $NIR(p)$ and $Red(p)$ are respectively the near infrared and red reflectance at a pixel p in the band. It is clear that NDVI values occupy the range [-1,1].

For areas with dense vegetation, NDVI has a high value (between 0.3 to 0.8) [10]. Other vegetation indices are also utilised to detect vegetation but NDVI is the most frequently used in remote sensing studies [37].

NIR radiation is strongly absorbed by water bodies and strongly reflected by soil and other surfaces. Furthermore, visible radiation (Red, Green, and Blue) is strongly reflected by water bodies. Normalized Difference Water Index (NDWI) utilizes these facts in a simple form as

$$NDWI(p) = \frac{Green(p) - NIR(p)}{Green(p) + NIR(p)} \tag{2}$$

where $NIR(p)$ and $Green(p)$ are respectively the near infrared and green reflectance at a pixel p in the band. The positive values of NDWI segregate open water bodies. The spectral response of water bodies indicates that the Green band is more suited towards segregating water features and keeping suitable ranges of NDWI as compared to Red and Blue bands [17, 27].

Its challenging to identify snow in satellite images because snow and clouds are equally bright in the visible wavelength. While snow cover absorbs Shortwave infrared (SWIR) radiation, clouds reflect SWIR radiation strongly. To utilize this difference in contrast between different bands, a normalized difference snow index (NDSI) is formulated [22]. NDSI utilizes these facts in a simple form as

$$NDSI(p) = \frac{Green(p) - SWIR(p)}{Green(p) + SWIR(p)} \tag{3}$$

where $Green(p)$ and $SWIR(p)$ are respectively the green and short-wave infrared reflectance at a pixel p in the band. Again, values range from -1 to 1. The threshold for determining the presence of snow varies and needs to be decided on a per-region basis.

2.3 Geospatial visualization

Time-varying data visualization is a well-studied area in information visualization of abstract data [15, 38]. Visualizing time-varying geospatial data is more challenging because of its location dependency [20].

Videos are commonly used to visualize changes in time-varying datasets. In [28], video synopsis has been used to reduce video size while retaining dynamic activities in a video. Google has created a timelapse tool using satellite imagery datasets to visualize changes in the Earth over past three decades [11]. In [25], the authors use videos to visualize changes in the Great Salt Lake. In general, the use of videos for visualizing these changes provides a sense of the overall trends but comparisons between consecutive frames is hard. For geospatial datasets, the comparison becomes harder, as the position of geospatial features in time is also important. The videos of time-varying geospatial data can be visualized on a physical globe for easy understanding [19].

To enable better frame comparison, multiple image lineups can be used [16, 39]. For example, multiple image lineups have been used to show changes in Lake Urmia over time [34]. To prepare the lineup, the authors use Moderate Resolution Imaging Spectroradiometer (MODIS) data [8] from 2000 to 2014. There are three disadvantages of the image lineup approach. First, the size of an individual image is decreased to accommodate all in a lineup. Second, only a limited number of frames can be placed in a lineup while still retaining the important details of a region. Third, it is hard to compare more than two images at a time in order to understand the changes occurring at a location.
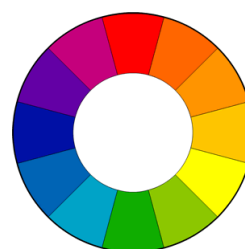

Figure 2: Basic color wheel [1].

Images can present and retain time-varying information in a single frame when using an appropriate color palette. An appropriate color-palette helps in logical organization of data and captures the trends and relationship within data. In addition to an appropriate palette, choosing the right number of colors for the color palette is an important aspect of identifying time-varying changes in Earth-features. In [23], two categories of color schemes, called sequential and diverging, were suggested. Furthermore, a low number of color palette is suggested for the proper representation of data classes in thematic maps. In sequential schemes, low data values are represented

by light colors and high data values are represented by dark colors. Sequential color schemes are used to represent data that changes from a high to low value. In diverging color schemes, the mid data value is represented using one color and two different sequential schemes diverge from this shared middle value. It is evidenced in [21] that palettes with fewer colors are more discriminable while more colors are harder for users to process.

The color wheel is a common tool used to design colors for a palette. Figure 2 shows one of the most commonly used wheels. Adjacent colors on the color wheel are called analogous colors. They are frequently found in nature and harmonize well to avoid jarring effects in the image [1, 18].

3 METHODOLOGY

The main goal of this work is to create a single image summary of Earth-features in a selected region that summarizes a certain duration of time. One challenge lies in how to capture changes in Earth-features. Another challenge is how to visualize these features. We use relevant bands from Landsat 8 datasets to create spectral indices that help in identifying the Earth-features. To visualize Earth-feature changes, we generate a recurrence map for the ROI and apply a color palette based on the recurrence of feature in any location. This leads to the generation of a SIS.

3.1 Capturing Earth-feature changes

Landsat 8 data can be accessed freely on Amazon Web Services (AWS) and Earthexplorer [6]. Earthexplorer only allows bulk data download for scenes, which results in long download times and more storage usage. We use AWS as the downloading source as it offers good speed and the option to download individual band data. AWS is also a suitable target for creating a web crawler because it provides a hyperlink for each file.

Landsat 8 images are separated into scenes for easy downloading. Each scene represents an area of approximately 185 km by 185 km and contains 11 bands and metadata files. The bands are delivered as 16-bit images in GeoTIFF file format. The hyperlinks for around 2 million Landsat 8 scenes are available in a file called *scene-list* that is provided by AWS. The file is updated daily with the latest scenes and each line in the file contains the details of the geographic location of the scene and a url for scene download.

We developed a downloader program that downloads scenes based on scene-list, date, bands, path, and row parameters. To download data in the range of 2013-2017 takes approximately an hour of time. After the downloading step, our system detects cloudy pixels using the Quality Assurance (QA) band provided by Landsat 8.

The QA band contains bit-packed information about the surface conditions, which helps to indicate clouds. If the decimal value of a pixel is above 31744, the pixel is likely to be cloudy [5].

Due to the non-spherical shape of the Earth and near-polar orbit of Landsat 8, different day scenes from the same region (identical path and row) are not exactly aligned. Exact alignment is crucial for temporal stacking of images.

Landsat 8 scenes are projected using the Universal Transverse Mercator projection system [7]. There is a linear mapping between the image coordinate (rows and columns) and the (geographical) UTM coordinate. Our system uses this linear mapping for the purpose of aligning images. The system uses the image and UTM coordinate system values from metadata files to align pixels for all layers from the ROI. The system loads all the referenced layers in memory for the spectral index calculation used to identify the feature of interest (Section 2.2).

The calculated value is compared to a threshold and, based on whether the spectral index value is above or below that threshold, the pixel at point p in each of the layers is classified as belonging to a feature. The threshold for identifying features depends on a number of factors, including the physical properties of observed features or the analyst making the observation [22, 27]. For example, values of NDWI greater than zero commonly indicate water. In our system, an appropriate threshold is decided for each region based on visual inspection. Note that the same threshold is used for all layers in a single region.
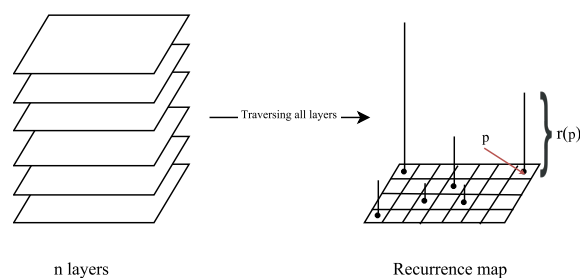

Figure 3: Recurrence map creation.

3.2 Recurrence map creation

After the stack of layers is classified into features, the recurrence map is prepared. A recurrence map represents the recurrence of a particular feature in the ROI. Our system has the capability to choose the ROI for the recurrence map preparation. For this research, the ROI is chosen to be inside the boundaries of a Landsat 8 scene. To better understand the recurrence map, n temporal layers in the image collection are considered. For each point p of the map, the repetition of the feature at p, $r(p)$, is stored in the recurrence map. Figure

3 illustrates the recurrence map. The value of $r(p)$, is normalized by the total number of non-cloudy layers at that point. The recurrence map can be constructed via a one time traversal of all layers in the current time range and stored. Once a recurrence map is created, various color maps can be used on it without the need to traverse all layers again.

3.3 Color-mapping

Our system follows a color-mapping procedure to apply a particular color-palette to the recurrence map in order to generate a SIS. Let us denote the current color palette by $c = \{c_1, ..., c_m\}$ where m is the number of colors. Each recurrence value is mapped to a color c_i (for some i). The color-palette and range of the recurrence map are also indicated in the SIS results. To provide a stronger distinction among feature categories, we choose palettes with a small number of colors [33]. Since the range of $r(p)$, is normally larger than m, a lookup table L is needed to assign a color to any $r(p)$

$$L: \quad r(p) \to c.$$

In our system, L is a uniform sampling of color maps by default. For practical case studies, one may tweak this transfer function to customize the result. Based on user preferences, our system can easily apply predefined sequential, divergent, and user-defined custom color-palettes to the recurrence map. We can also apply natural colors present in the RGB satellite images of the region. The color schemes for each of the case studies have been chosen in order to highlight the changes in features and maintain the context of surrounding regions.

4 CASE STUDIES

To evaluate our method and the implemented prototype, we have experimented on three case studies to highlight changes in Lake Urmia in north west Iran, the Amazon Rainforest in Brazil and the Bering Glacier in Alaska.

4.1 Lake Urmia

There has been a decrease in the water level of lake Urmia since the 1990s [4]. Some of the major speculated reasons for this decline are dam construction, diverting water for irrigation, less precipitation, and warmer climates [24]. There are many repercussions of this phenomenon. Reduction in water level is causing the salt levels to increase, thus causing the native brine shrimp population to decrease [14]. Since brine shrimp is the major food source for the bird population in this region, it is causing significant ecological disruption. The current increase in salt content is also causing the surrounding plant population to decrease as the drying of the lake also leaves a huge salt trail around the lake boundary.

In this section, SIS have been prepared for lake Urmia in order to observe the time-varying changes in water recurrence. A description of the area of study, choices of relevant spectral indices, and color palette are crucial elements of generating the summary images.

The study area is the Lake Urmia region in Iran lying between Urmia and Tabriz cities (as shown in Figure 1). According to the Landsat 8 operational orbit WRS-2 [13], scenes correspond to path 169 and row 34. Cloudy pixels in the dataset were detected using the QA band (as shown in Section 3.1). Positive values of NDWI are assumed to indicate the presence of water in this region. After classification of water in each layer, the recurrence map is prepared. In the next step a color-mapping is applied to the recurrence map. A color range from red to blue from the color wheel was used in order to represent Lake Urmia (as shown in Figure 2). Blue is assigned to the maximum recurrence value as water is typically represented as blue in pictures. Furthermore, a range of analogous colors and a variety of colors are used in order to represent close recurrences while at the same time distinguishing recurrences easily. Recurrences close to zero indicate feature absence and are assigned to a white color so that they don't distract one from observing nonzero feature presence. The objective is to maintain an intuitive understanding of the feature of interest with this color choice. Finally, the SIS is overlaid atop Google maps. In order to maintain a relevant location context in the SIS results, only important information such as roads, labels, and major city names have been kept. Figure 1 shows the result for Lake Urmia with a 12 color palette from a recurrence map created in the period 2013-2017.

There are some important observations evident from the result:

1. A desiccation in the wet region of the lake is clearly visible in the result. The inner region is blue while the boundary of the lake is colored otherwise. The upper part of Urmia has water present most of the time, as can be seen in the result image. Because of the difference in recurrence in the upper and lower parts, it looks like the lake could separate into upper and lower parts. Similar conclusions are obtained by combining elevation and surface water data from multiple sensors and satellites to track lake water level [34].

2. Another observation is the existence of several streams and rivers around the lake. It seems that they are important sources of water intake, however in the visualization they are usually presented in dark red. Dark red is assigned to places that rarely have water recurrence during the observation period. The limited sources of water inflow is one of the main reasons for the drying of lake over the years.

| (a) January | (b) February | (c) March | (d) April | (e) May | (f) June |

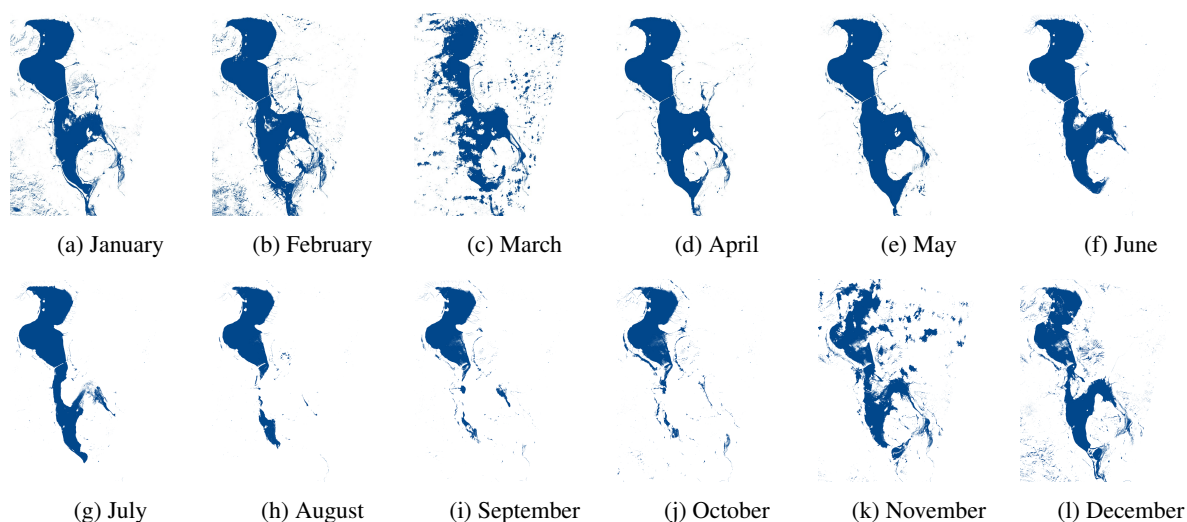| (g) July | (h) August | (i) September | (j) October | (k) November | (l) December |

Figure 4: Multiple image lineup of Lake Urmia from 2015.

3. The figure also shows that there is a large red area surrounding the lake boundary. The red color suggests that the region rarely has water present. In [32], it has been speculated that the boundary of the lake usually has salt deposits. Winds carry salt deposits to settlements near the lake which impacts vegetation and causes health problems for people living in these surrounding areas.

Here we discuss the advantages of SIS (Figure 1) over traditional methods of visualizing the layers frame-by-frame (timelapse or animation) or by placing them in a lineup (Figure 4).

- Only one layer at a time can be observed with the timelapse visualization, and the context of both previous and subsequent images are lost. With SIS, its possible to see all changes in the water recurrence over time without losing the context. The recurrence of a feature at p can be easily deciphered by the shade of color at p.

- Showing 12 layers as images side-by-side requires more space and, consequently, either the resolution of each layer has to be decreased or it needs to be presented on a larger screen. As the number of layers increase, both of the previous problems are exacerbated. The resolution of SIS is independent of the number of layers that need to be visualized. So, whether 89 layers or 12 layers are being visualized, the resolution of the summary image doesn't change.

- SIS captures the trends of changes happening in the region. By using SIS, one can evaluate how frequently a feature occurs in a region. The SIS with its color palette easily and immediately highlights
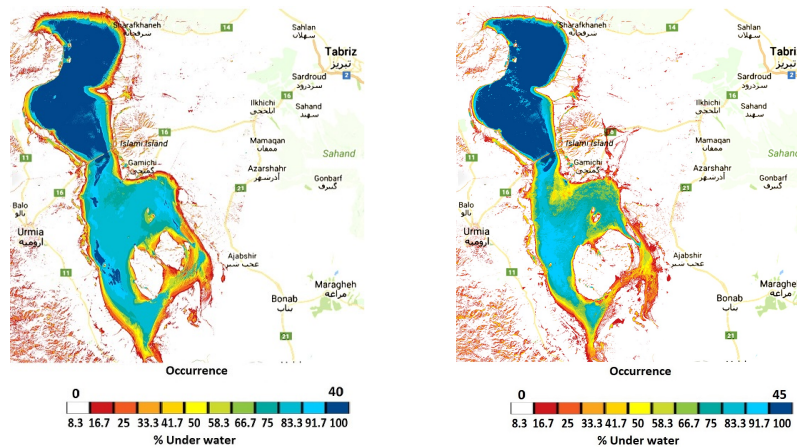
which regions have a permanent occurrence of a feature. An example is shown in Figure 1, where one can observe that the upper part of Lake Urmia always has water while the lower part has lesser occurrence.

4.1.1 Comparison of two SIS

Although using one SIS illustrates a number of time-varying changes, experiments were conducted to observe the benefits of comparing two SIS (as shown in Figure 5). In our experiments, comparisons of two different time periods were done and the results have been shown in Figure 5 On comparing Figure 5a and Figure 5b, the island area in white near the lower right of the image seems to be increasing in size from 2013-2014 to 2015-2016. The islands have almost merged in 2015-2016. The yellow area near Gamichi is increasing in area over time. This indicates less water recurrence and drying of the lake, providing clear support for the increased salt deposition in the area as mentioned in [32].

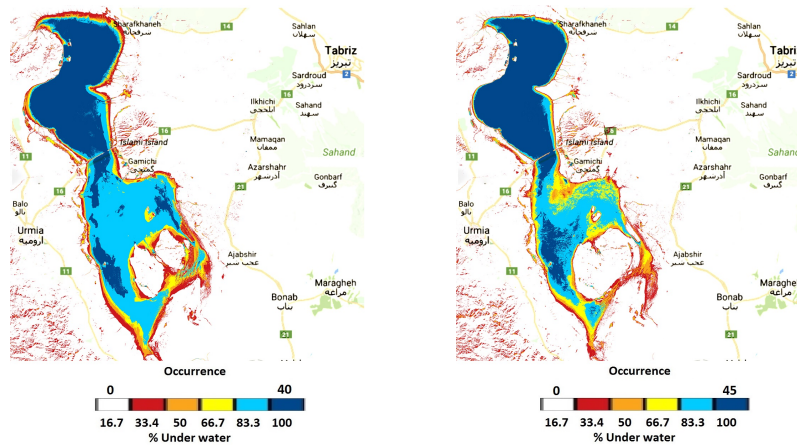### 4.1.2 Experimentation with different color counts

To test the impact of different color counts on results, summaries for 2 year durations have been prepared using a color palette with 6 colors (as shown in Figure 6). One can see similar trends in Figure 5 with 12 colors and Figure 6 with 6 colors. There are some advantages of using a larger number of colors. The color transition is smoother in case of 12 colors. The small number of colors in the palette can mask the underlying changes taking place in the region. For example, the difference between recurrences in the upper and lower parts of Urmia is more prominent in Figure 5b as compared to Figure 6b. There are some patchy deep blue colors that we observe in lower parts of Figure 6b because a wide range of recurrences have been assigned to a deep blue

ISSN 2464-4617(print)
ISSN 2464-4625(CD)

Computer Science Research Notes
CSRN 2801

Full Papers Proceedings
http://www.WSCG.eu

(a) 2013-2014

(b) 2015-2016

Figure 5: Experimental results with 12 colors.

(a) 2013-2014

(b) 2015-2016

Figure 6: Experimental results with 6 colors.

color so its possible to segregate these recurrences in Figure 5b but not in 6b. However, there are some disadvantages of choosing a large number of colors. Using a large number of colors increases redundant patterns in the images (red patches for low recurrences). Moreover, having a large number of colors can make it difficult to distinguish different recurrences.

4.2 Amazon Rainforest

Deforestation helps humans in some sense, but it has extreme negative impacts on climate change and the extinction of flora and fauna [12]. Brazil has recently made huge progress in reducing deforestation and in increasing reforestation [3]. As a result of this progress, heat trapping emissions have been lowered in Brazil as compared to other nations. The international effort known as "Reducing emissions from deforestation and forest degradation" (REDD+) contributed significantly to this achievement [9]. As part of this effort, developing nations reduce deforestation whilst wealthy nations compensate for economic loss. Norway pledged 2.5 billion

dollars for the effort and Brazil pledged to reduce the rate of deforestation drastically by 2020.

Rondonia, a state in Brazil, was the most deforested part of the Amazon ecosystem in recent decades [12]. To observe the vegetation trends in the region, a SIS for the region has been created using path 232 and row 68 of Landsat 8 data. A natural and sequential color-palette has been used to generate the SIS. For example, dense vegetation usually looks dark-green in nature as well as in satellite imagery. Thus, a palette of dark-green to white has been used in the Amazon Rainforest case to represent high to low recurrences. A similar palette is used by Google Earth for showing regions with live and dead vegetation. In a recent work, a similar palette was adopted to apply cell shading to terrain features in order to represent trees [18]. The color palette was sampled from the paintings of famous panorama maps artist Heinrich Berann in order to replicate his hand-drawn style.
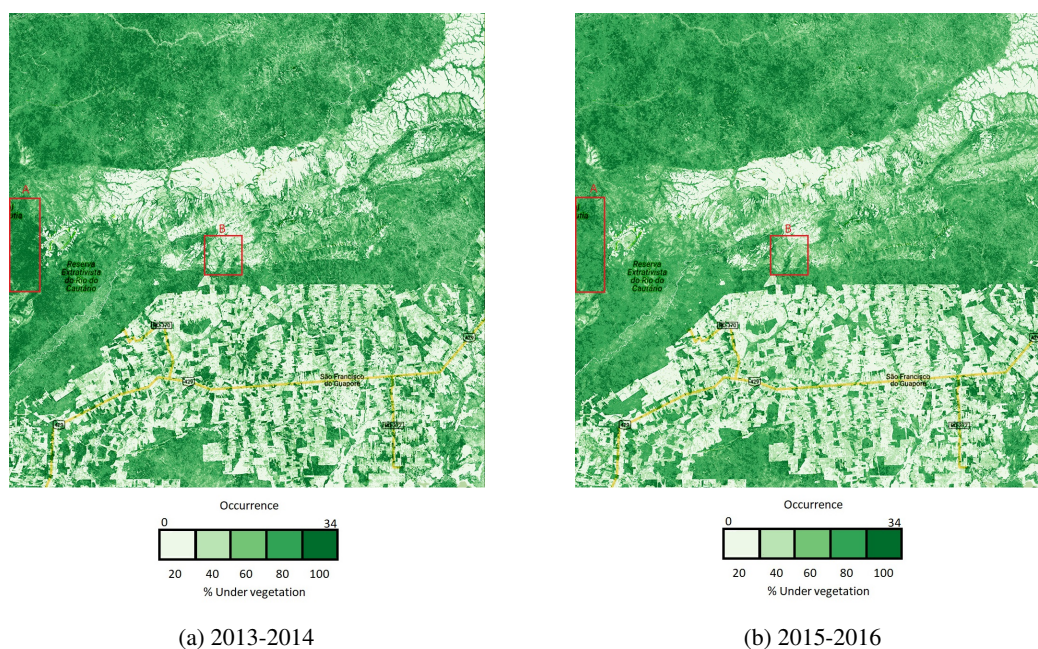
(a) 2013-2014

(b) 2015-2016

Figure 7: SIS for the Rondonia region (Amazon Rainforest).

The results are created using 34 layers from the duration of 2013-2014 and 34 layers from the duration of 2015-2016. On comparing Figure 7a and Figure 7b, one can observe that the amount of vegetation has generally decreased in the region. The dark green regions on left of Figure 7a have changed to light green in Figure 7b, which indicates decreased recurrence of vegetation (shown as A in Figure 7). White regions in the center have increased and green regions have decreased in Figure 7b when compared to Figure 7a, which again indicates a decrease in vegetation recurrence. In a few places, there is an increased recurrence too. These results suggest that the deforestation is still going on over the years (shown as A in Figure 7) while there has been some positive results from reforestation efforts (shown as B in Figure 7).

4.3 Bering Glacier

The Bering Glacier is one of the largest glaciers in North America and is located in Alaska. According to [2], the glacier has been retreating at an alarming rate of 10 miles per year. Ground measurements are hard to perform for glaciers due to the harsh conditions prevailing in glacial regions. Thus, remote sensing measurements make it easier to understand ongoing processes in glacial regions.

Using Landsat 8 data from 2013-2017 and Normalized Difference Snow index with an intuitive color palette, Figure 8 has been prepared. The results are shown in Figure 8. The scenes correspond to path 64 and row 18 and we use 5 colors to indicate the snow recurrence. 39 layers from 2013-2014 and 43 layers from 2015-2016 were used to prepare the SIS results. The green color

corresponds to very low values of snow recurrence. The cyan color in the bottom half of the image indicates the North Pacific ocean.

Most of the glacier region has snow present all around the observed duration, which is indicated by deep blue color. The image clearly shows the glacier retreating. The central medial moraine region [31] in the top left between the Bering and Steller Glaciers shows sparse and periodic snow cover (shown as A in Figure 8). On comparing Figure 8a to Figure 8b, it seems that the front of the Bering Glacier has retreated from 2013-2014 to 2015-2016. Furthermore, in 2015-2016, the occurrence of snow around the boundary of the glacier seems to be decreasing (vegetation-snow interface in Figure 8).

5 CONCLUSION

In this paper, we have explored the key aspects of generating single image summaries of Earth-features using Landsat 8 data. We have discussed techniques to identify Earth-features, detect and ignore clouds, reference layers, calculate recurrence of features, and apply a color palette to generate the result. We have presented results and discussed the implications of the results using different counts of colors and layers. We have shown the utility of summaries in detecting changes by describing case studies of several sample areas. Landsat 8 data was obtained from AWS for this research. Our results show change trends which are consistent with other studies and identify new trends which may be utilized by other researchers.

There is room for future work. Clouds hamper the ability to observe land cover in Landsat 8 and sometimes
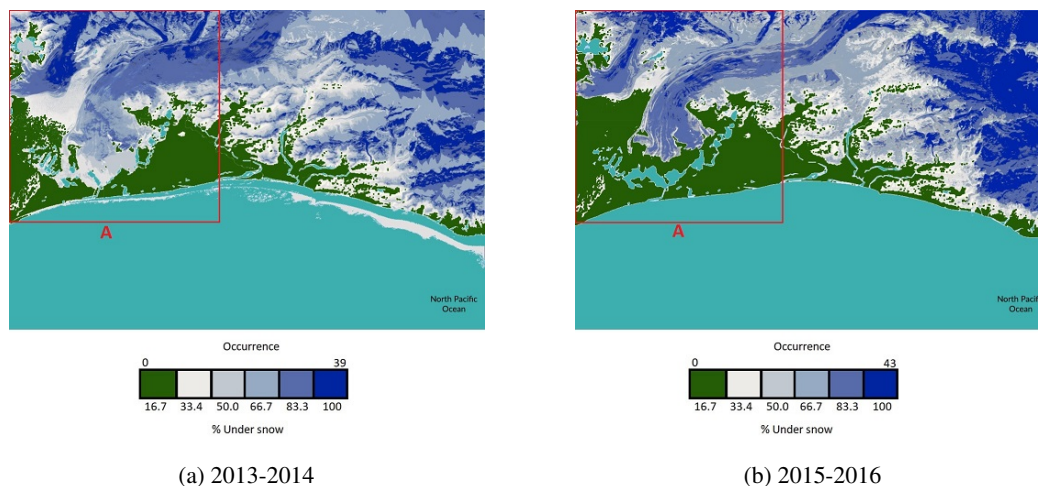
(a) 2013-2014

(b) 2015-2016

Figure 8: SIS for the Bering Glacier region.

bring noise into the results. An automatic method for reconstructing data that is hidden by clouds would generate better results. Additionally, it would be interesting to use Landsat 8 along with MODIS and other satellite imagery datasets. Although MODIS has a coarse spatial resolution, its fine temporal resolution of 1 day seems promising towards capturing the change trends.

6 ACKNOWLEDGMENTS

7 REFERENCES

[1] *Basic color schemes: Color theory introduction*, `http://www.tigercolor.com/color-lab/color-theory/color-theory-intro.htm`, (Accessed on 11/13/2017).

[2] *Bering glacier melts faster | far north science*, `http://www.farnorthscience.com/2007/06/04/climate-news/bering-glacier-melts-faster/`, (Accessed on 11/10/2017).

[3] *Brazil's success in reducing deforestation (2011)*, `https://www.ucsusa.org/global_warming/solutions/stop-deforestation/brazils-reduction-deforestation.html#.Wi7nPd-nFqR`, (Accessed on 12/11/2017).

[4] *Lake urmia: how irans most famous lake is disappearing-world news-the guardian*, `theguardian.com/world/iran-blog/2015/jan/23/`, (Accessed on 12/18/2017).

[5] *Landsat 8 pre-collection quality assessment band | landsat missions*, `https://landsat.usgs.gov/qualityband`, (Accessed on 01/15/2018).

[6] *Landsat data access | landsat missions*, `https://landsat.usgs.gov/landsat-data-access`.

[7] *Landsat processing details | landsat missions*, `https://landsat.usgs.gov/landsat-processing-details`, (Accessed on 11/12/2017).

[8] *Modis web*, `https://modis.gsfc.nasa.gov/data/`, (Accessed on 12/19/2017).

[9] *Redd+ - home*, `http://redd.unfccc.int/`, (Accessed on 12/11/2017).

[10] *Remote sensing phenology*, `https://phenology.cr.usgs.gov/ndvi_foundation.php`, (Accessed on 12/15/2017).

[11] *Timelapse : Google earth engine*, `https://earthengine.google.com/timelapse/`, (Accessed on 12/05/2017).

[12] *World of change: Amazon deforestation : Feature articles*, `https://earthobservatory.nasa.gov/Features/WorldOfChange/deforestation.php`, (Accessed on 12/11/2017).

[13] *The worldwide reference system « landsat science*, `https://landsat.gsfc.nasa.gov/the-worldwide-reference-system/`, (Accessed on 11/21/2017).

[14] M Abbaspour and A Nazaridoust, *Determination of environmental water requirements of lake urmia, iran: an ecological approach*, International Journal of Environmental Studies **64** (2007), no. 2, 161–169.

[15] Wolfgang Aigner, Silvia Miksch, Heidrun Schumann, and Christian Tominski, *Visualization of time-oriented data*, Springer Science & Business Media, 2011.

[16] Roger Beecham, Jason Dykes, Wouter Meulemans, Aidan Slingsby, Cagatay Turkay, and Jo Wood, *Map lineups: effects of spatial structure on graphical inference*, IEEE transactions on visualization and computer graphics **23** (2017), no. 1, 391–400.

[17] Dale HP Boland, *Trophic classification of lakes using landsat-1 (erts-1) multispectral scanner data*, US Environmental Protection Agency, Office of Research and Development, Corvallis Environmental Research Laboratory, Assessment and Criteria Development, 1976.

[18] S. Alex Brown and Faramarz Samavati, *Real-time panorama maps*, Proceedings of the Symposium on Non-Photorealistic Animation and Rendering (New York, NY, USA), NPAR '17, ACM, 2017, pp. 6:1–6:11.

[19] Shima Dadkhahfard, Katayoon Etemad, John Brosz, and Faramarz Samavati, *Area preserving dynamic geospatial visualization on physical globe*, 9th International Conference on Information Visualization Theory and Applications, IVAPP 2018, 2018.

[20] Jason Dykes, Alan M MacEachren, and M-J Kraak, *Exploring geovisualization*, Elsevier, 2005.

[21] Connor C Gramazio, David H Laidlaw, and Karen B Schloss, *Colorgorical: Creating discriminable and preferable color palettes for information visualization*, IEEE transactions on visualization and computer graphics **23** (2017), no. 1, 521–530.

[22] Dorothy K Hall and George A Riggs, *Normalized-difference snow index (ndsi)*, Encyclopedia of snow, ice and glaciers, Springer, 2011, pp. 779–780.

[23] Mark Harrower and Cynthia A. Brewer, *Colorbrewer.org: An online tool for selecting colour schemes for maps*, The Cartographic Journal **40** (2003), no. 1, 27–37.

[24] M Hoseinpour, A Fakheri Fard, and R Naghili, *Death of urmia lake, a silent disaster investigating causes, results and solutions of urmia lake drying*, 1st International Applied Geological Congress, Department of Geology, Islamic Azad University, Islamic Azad University-Mashad Branch, Iran, 2010.

[25] M.C. Hung and Y.H. Wu, *Mapping and visualizing the great salt lake landscape dynamics using multitemporal satellite images, 1972 to 1996*, International Journal of Remote Sensing **26** (2005), no. 9, 1815–1834.

[26] FJ Kriegler, WA Malila, RF Nalepka, and W Richardson, *Preprocessing transformations and their effects on multispectral recognition*, Remote Sensing of Environment, VI, 1969, p. 97.

[27] S. K. McFEETERS, *The use of the normalized difference water index (ndwi) in the delineation of open water features*, International Journal of Remote Sensing **17** (1996), no. 7, 1425–1432.

[28] A. Rav-Acha, Y. Pritch, and S. Peleg, *Making a long video short: Dynamic video synopsis*, 2006 IEEE Computer Society Conference on Computer Vision and Pattern Recognition (CVPR'06), vol. 1, June 2006, pp. 435–441.

[29] J_W Rouse Jr, RH Haas, JA Schell, and DW Deering, *Monitoring vegetation systems in the great plains with erts*, (1974).

[30] David P Roy, MA Wulder, TR Loveland, CE Woodcock, RG Allen, MC Anderson, D Helder, JR Irons, DM Johnson, R Kennedy, et al., *Landsat-8: Science and product vision for terrestrial global change research*, Remote Sensing of Environment **145** (2014), 154–172.

[31] Robert Allan Shuchman and Edward George Josberger, *Bering glacier: interdisciplinary studies of earth's largest temperate surging glacier*, vol. 462, Geological Society of America, 2010.

[32] Richard Stone, *Saving iran's great salt lake*, Science **349** (2015), no. 6252, 1044–1047.

[33] Alexandru C Telea, *Data visualization: principles and practice*, CRC Press, 2014.

[34] M.J. Tourian, O. Elmi, Q. Chen, B. Devaraju, Sh. Roohi, and N. Sneeuw, *A spaceborne multisensor approach to monitor the desiccation of lake urmia in iran*, Remote Sensing of Environment **156** (2015), no. Supplement C, 349 – 360.

[35] Stef van den Elzen and Jarke J van Wijk, *Small multiples, large singles: A new approach for visual data exploration*, Computer Graphics Forum, vol. 32, Wiley Online Library, 2013, pp. 191–200.

[36] M. M. Verstraete and B. Pinty, *Designing optimal spectral indexes for remote sensing applications*, IEEE Transactions on Geoscience and Remote Sensing **34** (1996), no. 5, 1254–1265.

[37] Andrés Viña, Anatoly A Gitelson, Anthony L Nguy-Robertson, and Yi Peng, *Comparison of different vegetation indices for the remote assessment of green leaf area index of crops*, Remote Sensing of Environment **115** (2011), no. 12, 3468–3478.

[38] Chaoli Wang, Hongfeng Yu, and Kwan-Liu Ma, *Importance-driven time-varying data visualization*, IEEE Transactions on Visualization and Computer Graphics **14** (2008), no. 6, 1547–1554.

[39] Hadley Wickham, Dianne Cook, Heike Hofmann, and Andreas Buja, *Graphical inference for infovis*, IEEE Transactions on Visualization and Computer Graphics **16** (2010), no. 6, 973–979.